

Migration and Final Location of Hot Super Earths in the Presence of Gas Giants

Ji-Lin Zhou¹ and Douglas N.C. Lin^{2,3}

¹ Department of Astronomy, Nanjing University, Nanjing 210093, China
email: zhoujl@nju.edu.cn

²UCO/Lick Observatory, University of California, Santa Cruz, CA 95064, USA
email: lin@ucolick.org

³Kavli Institute of Astronomy and Astrophysics, Peking University, Beijing 100871, China

Abstract. Based on the conventional sequential-accretion paradigm, we have proposed that, during the migration of first-born gas giants outside the orbits of planetary embryos, super Earth planets will form inside the 2:1 resonance location by sweeping of mean motion resonances (Zhou et al. 2005). In this paper, we study the subsequent evolution of a super Earth (m_1) under the effects of tidal dissipation and perturbation from a first-born gas giant (m_2) in an outside orbit. Secular perturbation and mean motion resonances (especially 2 : 1 and 5 : 2 resonances) between m_1 and m_2 excite the eccentricity of m_1 , which causes the migration of m_1 and results in a hot super Earth. The calculated final location of the hot super Earth is independent of the tidal energy dissipation factor Q' . The study of migration history of a Hot Super Earth is useful to reveal its Q' value and to predict its final location in the presence of one or more hot gas giants. When this investigation is applied to the GJ876 system, it correctly reproduces the observed location of GJ876d around 0.02AU.

Keywords. Planets and Satellites: Formation; Celestial Mechanics

1. Introduction

The search for habitable planets is an essential step in the quests to unravel the origin of the Solar System and find life elsewhere. To date, more than 250 exoplanets are detected mainly by radial velocity survey of nearby solar-type stars[†]. In the database, there are 17 planets with mass less than 25 Earth mass (M_{\oplus}), and among them 8 planets have orbits with period < 10 days. They are GJ876d, HD69830b, GJ674b, HD160691d, 55Cnc e, Gl581b, HD219828b and GJ436b. We call them ‘hot super Earths’.

According to the conventional core-accretion scenario of planet formation, planets form in a protoplanetary disk around the host protostar. Through the sedimentation of dust, cohesive collisions of planetesimals, many embryos will form by accreting and clearing the planetesimals in their feed zone (a band centered on the embryo with a width of ~ 10 Hill radius) and result in dynamically isolated bodies. In a disk with several (f_d) times of minimum mass solar nebular, the isolation mass is (Zhou et al. 2007),

$$M_{\text{iso}} = 0.51 \times 10^{-2} M_{\oplus} \eta k_{\text{iso}}^{3/2}, \quad (1.1)$$

where

$$\begin{aligned} \eta &= (f_d f_{\text{ice}})^{3/2} \left(\frac{a}{1\text{AU}}\right)^{3/4} \left(\frac{M_*}{M_{\odot}}\right)^{-3/2}. \\ \log(k_{\text{iso}}) &= \sqrt{b^2 + 0.61c} - b, \\ b &= 2.8 + 0.33 \log \eta, \\ c &= 3.6 + 0.67 \log \eta + \log T_{\text{dep}}, \end{aligned} \quad (1.2)$$

[†] <http://vo.obspm.fr/exoplanetes/>, <http://exoplanets.org/>.

$f_{\text{ice}} = 1$ for embryos inside the ice line and $f_{\text{ice}} = 4.2$ outside that, T_{dep} is the timescale of depletion of gas disk.

According to equation (1.1), the isolation mass inside the ice line ($a \approx 2.7\text{AU}$ in solar system) is too small to become a super Earth. Unless their nascent protostellar disks are highly compact, the observed super Earths are unlikely formed in situ. Some extra mechanisms are required to account for the excitation of eccentricity and the merge of isolated embryos into super Earths. In Zhou et al. (2005), we have proposed two mechanisms that may lead to the excitation of eccentricities of embryos: (1) During the type-II migration of a first-born gas giant planet outside the orbits of embryos, the locations of its mean motion resonances (mainly 2:1 resonance) sweep through the embryos region; (2) During the dispersal of the gas disk, the location of secular resonance between the gas giant and embryos sweeps through the inner orbits. Additional mechanisms have also been discussed by Raymond et al. (2007).

In this paper, we suppose a super Earth has formed through one of the above mechanisms, and study the subsequent evolution after the gas disk was depleted and the gas giant has stopped its migration. First we briefly review the secular evolution of two planets under tidal dissipation. Then we show some numerical results in section 3. Conclusions are presented in section 4.

2. Secular dynamics under tidal dissipation

2.1. Tidal perturbation timescale

We adopt a two-planet system as a model. Suppose two planets with mass m_i ($i = 1, 2$) (in the order from inner to outer) moving around a star with mass m_* in the same orbital plane. Let m_1 be an Earth-like planet, and m_2 a gas giant, S_i, Ω_i, a_i, r_i are the radius, spin rate (with spin axis perpendicular to the orbital plane), semi major axis, distance from the star of planet i ($i = 1, 2$ respectively), . The acceleration to the relative motion of m_i caused by the tidal interaction between the star and planet m_i has the form of (Mignard 1979, Mardling & Lin 2002)

$$\mathbf{F}_{i,\text{tid}} = -(1 + \lambda^{-1}) \frac{9n_i}{2Q'_i} \left(\frac{m_*}{m_i}\right) \left(\frac{S_i}{a_i}\right)^5 \left(\frac{a_i}{r_i}\right)^8 [3v_{ir}\hat{r} + (v_{i\phi} - r_i\Omega_i)\hat{\phi}], \quad (2.1)$$

where $\hat{r}, \hat{\phi}$ are the unit vector of radial and transversal direction of the orbital plane, $\mathbf{V}_i = v_{ir}\hat{r} + v_{i\phi}\hat{\phi}$ and n_i are the Kepler velocity and mean motion of planet i ($i=1,2$), respectively, Q'_* and Q'_i are the effective tidal dissipation factor of the star and planet i defined as $Q' = 3Q/(2k_L)$, where $Q^{-1} = \tan(2\epsilon)$ is the effective dissipation function, ϵ is the tidal lag angle (Goldreich & Soter 1966), k_L is the Love number or twice the apsidal constance for gaseous planets (e.g., Mardling & Lin 2002), and

$$\lambda = \left(\frac{Q'_*}{Q'_i}\right) \left(\frac{m_*}{m_i}\right)^2 \left(\frac{S_i}{S_*}\right)^5 \quad (2.2)$$

is the ratio of tidal dissipation in the planet to that in the star. If $\lambda \gg 1$, tidal dissipation in the planet dominates the evolution.

The values Q'_* inferred from the observation of circularization period in various stellar clusters are $\sim 1.5 \times 10^5$ for young stars with age less than 0.1Gyr, and $\sim 10^6$ for mature stars (Terquem et al. 1998, Dobbs-Dixon et al. 2004). The Q' value for Jupiter inferred from Io's orbit evolution ranges from 5×10^4 to 2×10^6 (Yoder & Peale 1981). And for Earth, $Q'_E \approx 60$ (Yoder 1995). Thus for a gas giant planet with Jupiter mass, suppose $Q'_* \approx Q'_J = 10^5$, from Eq.(2.2), $\lambda \sim 10$, while for a terrestrial planet with Earth mass,

$\lambda \sim 10^4$. So in the case of tidal interaction between an Earth-like planet and a star, tidal dissipation in the planet dominates the evolution, thus we neglect the contribution of tide in star in the following study.

Take m_1 as an example. Under the perturbation of tidal effect, the averaged equations (over a period of orbital motion) governing the evolution of planet m_1 are,

$$\begin{aligned} \langle \dot{a}_1 \rangle_{\text{tide}} &= -2a_1\tau_{\text{tide}}^{-1} \left[f_1(e_1) - \left(\frac{\Omega_1}{n_1}\right)f_2(e_1) \right], \\ \langle \dot{e}_1 \rangle_{\text{tide}} &= -9e_1\tau_{\text{tide}}^{-1} \left[f_3(e_1) - \frac{11}{18}\left(\frac{\Omega_1}{n_1}\right)f_4(e_1) \right], \\ \langle \dot{\varpi}_1 \rangle_{\text{tide}} &= \langle \dot{\lambda}_1 \rangle_{\text{tide}} = 0. \end{aligned} \quad (2.3)$$

where ϖ_1, λ_1 are the longitude of perihelion and mean longitude of the orbit of m_1 (with volume density ρ_1), respectively, and

$$\tau_{\text{tide}} = \frac{4Q'_1}{63n_1} \left(\frac{m_1}{m_*}\right) \left(\frac{a}{S_1}\right)^5 = 2.4 \times 10^7 Q'_1 \left(\frac{a_1}{0.1\text{AU}}\right)^{\frac{13}{2}} \left(\frac{m_*}{m_\odot}\right)^{-\frac{3}{2}} \left(\frac{m_1}{m_\oplus}\right)^{-\frac{2}{3}} \left(\frac{\rho_1}{3\text{g cm}^{-3}}\right)^{\frac{5}{3}} \text{ yr}. \quad (2.4)$$

Functions used are:

$$\begin{aligned} f_1(e) &= (1 + \frac{31}{2}e^2 + \frac{255}{8}e^4 + \frac{185}{16}e^6 + \frac{25}{64}e^8)/(1 - e^2)^{15/2}, \\ f_2(e) &= (1 + \frac{15}{2}e^2 + \frac{45}{8}e^4 + \frac{5}{16}e^6)/(1 - e^2)^6, \\ f_3(e) &= (1 + \frac{15}{4}e^2 + \frac{15}{8}e^4 + \frac{5}{64}e^6)/(1 - e^2)^{13/2}, \\ f_4(e) &= (1 + \frac{3}{2}e^2 + \frac{1}{8}e^4)/(1 - e^2)^5, \\ f_5(e) &= (1 + 3e^2 + \frac{3}{8}e^4)/(1 - e^2)^{9/2}, \\ f_6(e) &= (1 + \frac{15}{2}e^2 + \frac{67}{14}e^4 + \frac{85}{32}e^6 + \frac{255}{448}e^8 + \frac{25}{1792}e^{10})/(1 + 3e^2 + \frac{3}{8}e^4), \\ f_7(e) &= (1 + \frac{45}{14}e^2 + 8e^4 + \frac{685}{224}e^6 + \frac{255}{448}e^8 + \frac{25}{1792}e^{10})/(1 + 3e^2 + \frac{3}{8}e^4). \end{aligned} \quad (2.5)$$

The evolution of spin rate Ω_1 is subjected to,

$$I_1 \dot{\Omega}_1 = -\frac{m_* m_1}{m_* + m_1} \mathbf{r}_1 \times \mathbf{F}_{1,\text{tide}} \quad (2.6)$$

where $I_1 \approx \frac{2}{5}m_1 S_1^2$ is the inertial momentum of m_1 . The averaged change rate is

$$\langle \dot{\Omega}_1 \rangle_{\text{tide}} = \frac{5}{2} \tau_{\text{tide}}^{-1} \left(\frac{a_1}{S_1}\right)^2 \left[f_2(e_1) - \left(\frac{\Omega_1}{n_1}\right)f_5(e_1) \right]. \quad (2.7)$$

A stable equilibrium configuration occurs at

$$\Omega_{1,\text{eq}} = \frac{f_2(e_1)}{f_5(e_1)} n_1. \quad (2.8)$$

Since the timescale to reach the equilibrium state ($\sim \tau_{\text{tide}}(S_1/a_1)^2$) is several orders less than the tidal circularization timescale, we suppose such a state is reached. Substitute Eq.(2.8) into (2.3), we derive the timescales of tidal evolution of m_1 ,

$$\tau_{a-\text{tide}} \equiv \frac{a_1}{\dot{a}_1} = -\frac{(1 - e_1^2)^{15/2}}{2e_1^2 f_6(e_1)} \tau_{\text{tide}}, \quad \tau_{e-\text{tide}} \equiv \frac{e_1}{\dot{e}_1} = -\frac{(1 - e_1^2)^{13/2}}{f_7(e_1)} \tau_{\text{tide}}. \quad (2.9)$$

Note that, $\tau_{a-\text{tide}} \gg \tau_{e-\text{tide}}$ when $e_1 \approx 0$. However, when $e_1 \approx 1$, $\tau_{a-\text{tide}}$ and $\tau_{e-\text{tide}}$ could be very small, and $\tau_{a-\text{tide}} < \tau_{e-\text{tide}}$ as long as $e > 0.63425\dots$

Due to the huge difference of Q' between the Earth-like planet m_1 and the gas giant m_2 , for our later investigation of tidal evolution with $a_1 < 0.63a_2$, we neglect the tidal effect in planet m_2 .

2.2. Secular evolution in the case of $e_1 \ll e_2$

When $e_1 \ll e_2$, the secular evolution of m_1, m_2 under tidal dissipation and general relativity effect can be approximated by the following equations (Mardling 2006):

$$\begin{aligned}\dot{e}_1 &= -W_o e_2 \sin \eta - W_T e_1, \\ \dot{e}_2 &= W_c e_1 \sin \eta, \\ \dot{\eta} &= W_q - W_o \left(\frac{e_2}{e_1}\right) \cos \eta,\end{aligned}\quad (2.10)$$

where $\eta = \varpi_1 - \varpi_2$, $\alpha = a_1/a_2$, $\beta = \sqrt{1 - e_2^2}$, and

$$\begin{aligned}W_o &= \frac{15}{16} n_1 \left(\frac{m_2}{m_*}\right) \alpha^4 \beta^{-5}, \\ W_T &= \tau_{e-tide}^{-1}, \quad W_c = \frac{15}{16} n_2 \left(\frac{m_1}{m_*}\right) \alpha^3 \beta^{-4}, \\ W_q &= \frac{3}{4} n_1 \left(\frac{m_2}{m_*}\right) \alpha^3 \beta^{-3} [1 - \sqrt{\alpha} \left(\frac{m_1}{m_2}\right) \beta^{-1} + \gamma \beta^3],\end{aligned}\quad (2.11)$$

with $\gamma = 4(n_1 a_1 / c)^2 (m_* / m_2) \alpha^3$, the ratio of general relativity to quadruple contribution of $\dot{\eta}$. According to these equations, the secular evolution of e_1 and e_2 mainly passes three stages:

(1) After a short time oscillation, the evolution of e_1 and η reaches a state of librating around a quasi-equilibrium configuration with $e_1 = e_1^{eq}$ and $\eta = 2n\pi$ or $(2n+1)\pi$, where (Mardling 2006)

$$e_1^{eq} = e_2 \frac{W_o}{|W_q|} = \frac{5/4\alpha e_2}{\beta^2 |1 - \sqrt{\alpha} (m_1/m_2) \beta^{-1} + \gamma \beta^3|}. \quad (2.12)$$

(2) As η librates and e_1 evolves to $e_1 = 0$ gradually, a_1 is damped according to Eq.(2.9), thus m_1 migrates inward efficiently.

(3) Finally e_2 is damped on a timescale $\tau_c \gg \tau_{e-tide}$. During this timescale, the orbit of m_1 is almost circularized, and migration of m_1 is effectively stopped at a location a_{1f} .

The location of a_{1f} is what we want to find. However, due to the presence of resonant motion, the evolution of the two-planet system in real situation is more complicated, as we will show below.

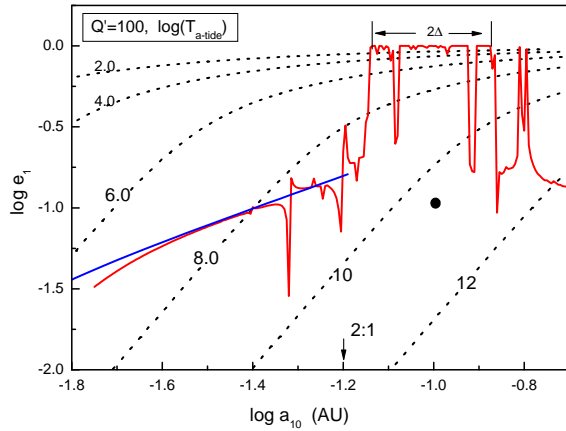


Figure 1. Maximum eccentricity (red solid line) of m_1 in an initial circular orbit of semi-major axis a_{10} excited by m_2 (black circle, with $a_{20} = 0.1\text{AU}$, $e_{20} = 0.1$). The black dotted lines with labels 2.0, 4.0, ... denote the timescale ($\log(T_{a-tide}/\text{years})$) of m_1 from Eq. (2.9) at the specific location of (a_{10}, e_1) with $Q'_1 = 100$. The blue dashed line is obtained by two times of the equilibrium values defined by Eq.(2.12).

3. Numerical simulations

We study the migration of an Earth-like planet under the tidal and mutual planetary perturbations with general three-body model. The system consists of a solar mass host star ($m_* = 1M_\odot$), an Earth-like planet with mass ($m_1 = 5M_\oplus$), and a Jupiter mass gas giant ($m_2 = M_J$, where M_J is Jupiter mass). Let m_1 be initially in a nearly circular orbit ($e_{10} = 10^{-3}$), and m_2 with initial elements $a_{20} = 0.1\text{AU}$, $e_{20} = 0.1$. To shorten the integration time, we let $Q' = 0.02$, as the migration timescale is proportional to Q' .

By integration of the full equations of the general three-body system without tidal dissipation, we plot the maximum eccentricity ($e_{1\text{max}}$) of m_1 excited by m_2 in Figure 1. The corresponding tidal-damping timescale obtained from equation (2.9) with (a_{10}, e_1) is also shown in the background of Fig.1.

As we can see from Figure 1, the orbits of m_1 at most locations with $a_{10} < 0.16\text{AU}$ have $T_{\text{a-tide}} < 10\text{Gyr}$. However, most of those orbits in the Hill unstable region around m_2 with half width $\Delta = (e_{20} + 2\sqrt{3}h)a_2 \approx 0.034\text{AU}$ (where $h = [m_2/(3m_*)]^{1/3}$) will be scattered to far away in our coplanar model. According to Zhou et al. 2005, embryos formed inside the location of the 2 : 1 resonance ($a_{2:1} \approx 0.063\text{AU}$) with m_2 are dynamically stable, so we focus on the evolution of orbits with initial semi major axis $a_{10} \leq 0.063\text{AU}$.

If planet m_1 is initially located in lower order mean motion resonances with m_2 , its eccentricity will be excited, thus a fast inward migration of m_1 is induced, according to Eq. (2.9). Fig. 2 shows the evolution of two orbits either from 2 : 1 resonance location ($a_{10} = 0.063\text{AU}$) or from non-resonance location ($a_{10} = 0.040\text{AU}$). During the subsequent passage through 5 : 2 resonance, the amplitude of eccentricity excitation is relatively large. Recall that, according to Eq. (2.9), the a -damping timescale is much smaller than that of e -damping at high eccentricity. Thus a fast migration occurs until e_1 decrease to a small value ~ 0.01 (Novak *et al.* 2003). Then a slow migration linked with the secular dynamics occurs, with $\eta = \varpi_1 - \varpi_2$ librating along an equilibrium value (see Fig.2b).

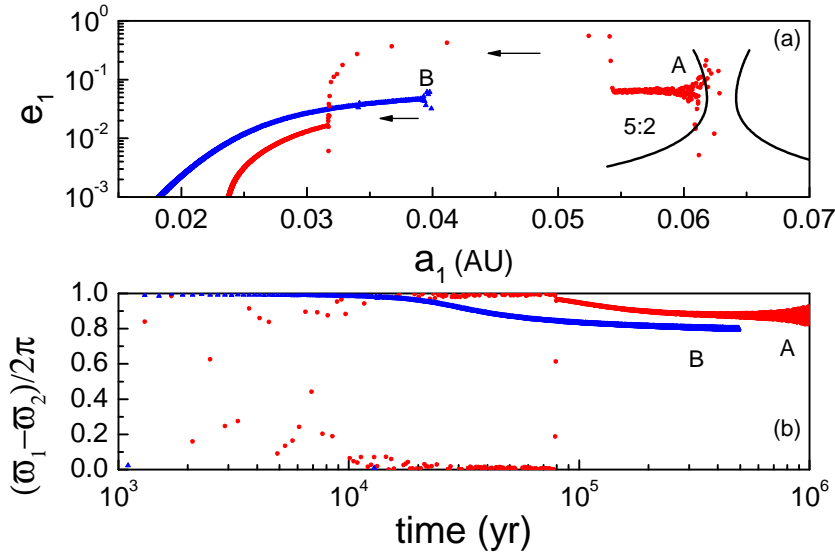


Figure 2. Evolution of orbits with $a_{10} = 0.063$ (orbit A) and $a_{10} = 0.040$ (orbit B). (a) Evolution track in $a_1 - e_1$ plane. The dashed line shows the width of 2 : 1 resonance obtained from the circular restricted-three-body problem. The 5 : 2 indicates the 5 : 2 resonance location at the place that the eccentricity of orbits A jumps up. The arrows indicate the evolution directions. (b) Evolution of $(\varpi_1 - \varpi_2)/2\pi$ (in radian).

The migration induced by resonant eccentricity-excitation is different from that excited by mutual secular perturbation. When we check the evolution of $a_i, e_i, (i = 1, 2)$ during the passage of 5 : 2 resonance, we find that a_1, e_1, e_2 have dramatic decrease after the crossing the 5 : 2 resonance (Fig.3). The decrease of e_2 causes the different final states (i.e., the final state of orbit A and B) in (a_1, e_1) plane of Fig.2. The final location is around $0.018 \sim 0.025\text{AU}$, depending on the different evolutionary routines.

In order to show that the above track correctly reproduces the observed location of extrasolar planets, we applied this study to the GJ876 system. GJ876 is a M dwarf star located 4.72 pc away from us in the solar neighborhood. To date, two gas giant planets, GJ876b and GJ876c, were observed to be located on orbits with period around 30 days and 60 days, an example of 2:1 mean motion resonance, and a hot planet GJ876d with mass around $5.7M_{\oplus}$ in an orbit with period 1.94 days ($a = 0.0208\text{AU}$, $e=0$). We numerically simulate the evolution of an Earth-like planet inside a gas giant located in the present orbit ($a_{20} = 0.13\text{AU}$, $e_{20} = 0.2243$). Figure 4 shows the evolution track of m_1 . The final location is around 0.02 AU according to the simulation, which is almost independent of the initial location of m_1 .

4. Summary and discussions

Many super Earths are observed to be located inside the orbits of gas giants. These super Earth and gas giant pairs may be a natural consequence of planet formation and migration. Embryos formed prior and interior to the gas giants are induced to migrate, collide, and evolve into close-in Super Earths (Zhou et al. 2005). In this report, we have shown that, the migration of super Earths under tidal dissipation and the perturbation from gas giants is mainly along the secular evolution paths. Although resonances be-

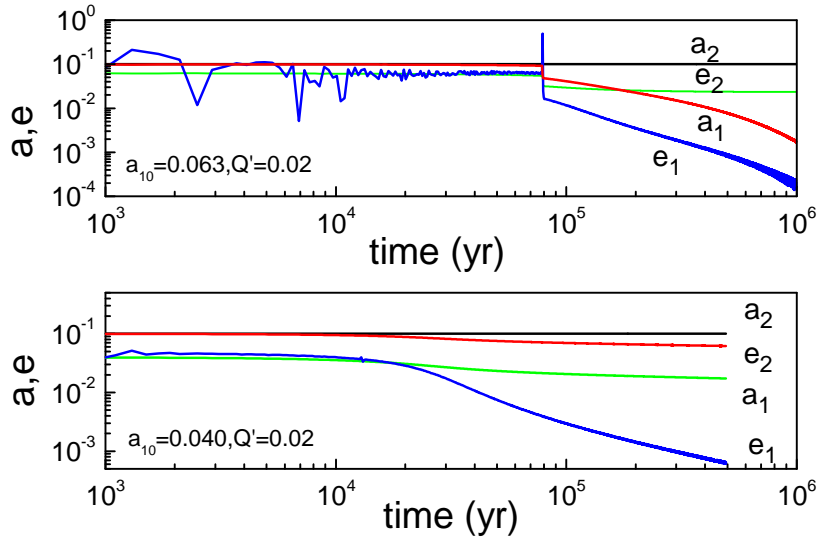


Figure 3. Evolution of orbital elements for the two orbits shown in Fig.2 with initial elements $a_{10} = 0.040, 0.063$, respectively. The evolution of orbit with $a_{10} = 0.040$ fits with the secular evolution described in section 2, but for the orbit with $a_{10} = 0.063$, the presence of the resonance leads to a dramatic increase (decrease) of $e_1(e_2)$ at time $t \approx 8 \times 10^4$ year, when the orbit crosses the 5:2 resonance in Fig.2.

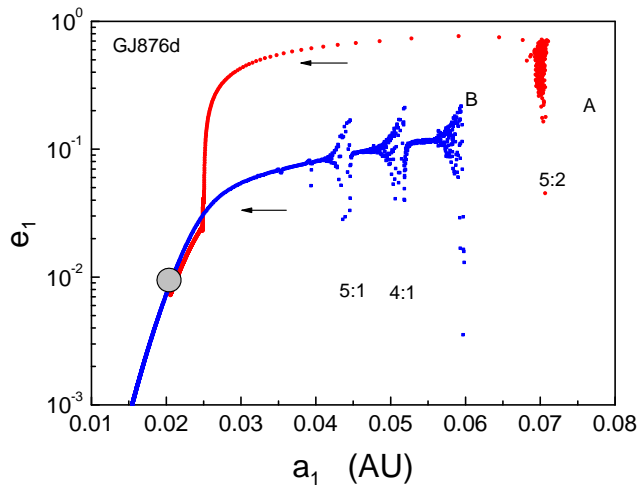


Figure 4. Evolution track of orbits with $a_{10} = 0.07074$ (the location of 5 : 2 resonance, orbit A) and $a_{10} = 0.060$ (orbit B). The arrows indicate the evolution directions.

tween super Earths and gas giants may excite the eccentricity and speed the migration timescale, the final evolution path can be well determined.

According to the investigation of this paper, we find that the study of the evolution path provides useful information in the following ways: (i) the migration path shows the evolution history, especially the evolution of e_1 , e_2 , a_1 (Figs.2,4). (ii) Comparing the observed location of the planet in the path, we can deduce the range of Q' values for the hot Super Earths. We will investigate in more details on these topic in the future.

Acknowledgements

This work is supported by NSFC(10778603,10233020), National Basic Research Program of China(2007CB814800), NASA (NAGS5-11779, NNG04G-191G, NNG06-GH45G), JPL (1270927), NSF(AST-0507424, PHY99-0794).

References

- Dobbs-Dixon, I., Lin, D. N.C. & Mardling, R. 2004, *ApJ*, 610, 464
 Goldreich, P.& Soter, S. 1966, *Icarus*, 5,375
 Ida, S., & Lin, D. N. C. 2004, *ApJ*, 604, 388
 Mardling, R. 2007, *MNRAS*(submitted), arXiv:0706.0224.
 Mardling, R., & Lin, D. N.C. 2004, *ApJ*, 573, 829
 Mignard, F. 1979, *The Moon and the Planets*, 20, 301
 Novak, G.S., Lai, D. & Lin, D.N.C. 2003, in *Scientific Frontiers in Research on Extrasolar Planets*, eds D. Deming & S. Seager, (San Francisco:ASP), 177
 Raymond S., Barnes, R., Mandell A.M. 2007, arXiv:0711.2015.
 Terquem,C. Papaloizou,J.C.B.,Nelson,R.P., & Lin, D.N.C. et al. 1998, *ApJ*,502,788.
 Yoder C.F. 1995 in *Global Earth Physics, A Handbook of Physical Constants*, ed. T. Ahrens (American Geophysical Union ,Washington)
 Zhou, J.L., Aarseth, S. J., Lin, D. N. C., & Nagasawa, M. 2005, *ApJ*, 631, L85
 Zhou, J.L., Lin, D.N.C.& Sun Y.S. 2007, *ApJ*, 666, 423